Joint EPRI – 123HiMAT International Conference on
Advances in High Temperature Materials
October 21–24, 2019, Nagasaki, Japan
J. Shingledecker, M. Takeyama, editors
https://doi.org/10.31339/asm.cp.am-epri-2019p0694

STUDY ON THE MAGNETIC NONDESTRUCTIVE TESTING TECHNOLOGY FOR OXIDE SCALES

Jingyi Du, Kang Chen, Jiacheng Wang, Le Hao
School of Electrical and Control Engineering, Xi'an University of Science and Technology, Xi'an (710054), China

Yue Qiao, Weizhong Teng, Ming Feng, Qingli Liu, Aijun Yan*
Xi'an Thermal Power Research Institute Co., Ltd., Xi'an (710054), China

ABSTRACT

The spalling of oxide scales at the steam side of superheater and reheater of ultra-supercritical unit is increasingly serious, which threatens the safe and economic operation of the boiler. However, no effective monitoring method is proposed to provide an on-line real-time detection on the spalling of oxide scales. This paper proposes an on-line magnetic non-destructive testing method for oxide granules. The oxide scale-vapor sample from the main steam pipeline forms liquid-solid two-phase flow after the temperature and pressure reduction, and the oxide granules are separated by a separator and piled in the austenitic pipe. According to the difference of the magnetic features of the oxide scales and the austenitic pipe, the oxide granule accumulation height can be detected through the spatial gradient variations of the magnetic induction. The laboratory test results show that the oxide scale accumulation can be accurately calculated according to the spatial gradient changes around the magnetized oxide granules, with the detection error not exceeding 2%.

KEY WORDS: Ultra-Supercritical Boiler; On-Line Separation; Oxide Scales; Magnetic Induction; Detection

INTRODUCTION

With the wide-range use of the ultra-supercritical coal-fired generator unit, the corrosion caused by steam oxidation of the high-temperature heating surface pipes on the boiler side is also increasingly serious. The oxide scale produced by high-temperature steam oxidation generally causes safety problems for the unit, including large-scale spalling and clogging of oxide scales, and even causing pipe bursting due to overtemperature and steam valve jamming due to high temperature. Not only that, the oxide granules enter the turbine along with the steam, which causes turbine blades to be eroded by the solid particles [1-3].

At present, the power plant generally detect the oxide scale problems of pipe sections of the superheater and reheater during the unit shutdown and maintenance. The detection may be performed by the ultrasonic testing, magnetic testing, radiographic testing, pipe-cutting inspection etc.. Ultrasonic testing is to test the growth thickness of the oxide scale which is not separated from the pipe wall at the initial formation stage based on the echo principle of the pipe wall interface [4]. Radiographic testing is to image the ray absorption of the oxide granules, thereby observing the accumulation of oxide granules

[5, 6]. The magnetic testing is to check whether the oxide scales exists or the accumulation of the oxide scales by measuring the magnetized oxide scale signals in the measuring tube through the outside of the paramagnetic Austenitic pipe [7, 8]. Due to the defects of the "shutdown testing", the above methods cannot detect the spalling of oxide scales on the line, so that it is impossible to give instructions promptly and prevent large-scale shedding and clogging of oxide scales. In addition, the oxide scale treatment by pipe-cutting cleaning and large-area pipe replacement is expensive with large workload, which increases the maintenance cost of the power plant. Therefore, it is of great significance to realize on-line monitoring of the spalling of oxide scales during the start-stop and operation of the unit.

The PAC detection system with the American generator unit enables on-line monitoring of spalling of oxides in the boiler steam-water system of the generator unit. The system realizes the monitoring of the spalling of oxide scales in the steam by detecting the vibration impact signal of the specific sensor during the movement of the oxide scales, but a great hidden danger exists in the equipment safety due to the erosion and abrasion of the probe caused by the solid particles [9-11]. At present, there are no effective application examples of online monitoring of spalling of oxide scales in China [12, 13].
In order to evaluate the spalling of oxide scales in the boiler steam-water system for the generator unit during the operation of the boiler, this paper proposes an on-line monitoring method for scale granules by cooling the steam-oxide scale vapor-solid two-phase flow at the high temperature and pressure and making the oxide granules separated from the cooled water and piled in the Austenitic pipe. According to the difference of the magnetic features of the oxide scales and the Austenitic pipe, the oxide granule accumulation height can be detected through the gradient changes of the spatial magnetic induction.

ONLINE SAMPLING SYSTEM FOR OXIDE GRANULES

When the main steam temperature and pressure of the supercritical boiler reach 540 °C/22 MPa or above, the conventional detection system cannot detect the oxide scales in the main steam pipe and the superheater pipe under high temperature and pressure. The on-line monitoring system for oxide granules herein makes the oxide scale-vapor sample of the main steam pipeline form a liquid-solid two-phase flow after the temperature and pressure reduction, causes the oxide granules separated and deposited from the water through the separator, and measures the oxide scale accumulation height and the granularity of small granules.
The structure of the online sampling system for oxide granules is shown in Fig. 1. The online sampling pipeline system is located between the superheater and the steam turbine and is connected to the main steam pipeline, and is composed of a high temperature and high pressure frame, a magnetic sensing device, a manual sampling area and an instrument monitoring area. The high temperature and high pressure frame mainly introduces and cools the sample vapor, and converts the gas-solid two-phase flow into a liquid-solid two-phase flow for further analysis. Sampling and cooling of the steam sample is ongoing and the cooling efficiency of the steam sample is fixed. The magnetic sensitivity detecting device measures the cumulative height of the large scale oxide scale during operation by using the magnetic properties of the scale, and determines the amount of scale in the steam by the height change, and estimates the steam tube according to the amount of scale particles in the partial steam sample. The oxide particles that flow through the whole process further speculate on the overall generation

of the scale particles. The manual sampling area provides subsequent instrumentation measurements by reducing the pressure of the high pressure water sample and provides overpressure protection under high pressure to provide filtration, decompression and overpressure protection. The instrument monitoring area is to monitor the pressure flow in the pipeline to prevent the temperature or pressure from exceeding the alarm value and to protect personnel and equipment. After treatment by the cooler, the high temperature and high pressure steam is condensed into liquid water, the temperature and pressure monitoring points are set, and the temperature and pressure are monitored. When the high pressure liquid water carries the oxide particles flowing through the separator, large oxide particles are deposited at the bottom of the separator. An on-line detection device for oxide particles detects the cumulative height of oxide particles at the bottom of the separator in real time. The separator is not directly connected to the steam delivery pipe, but is connected to the high temperature and high pressure frame and the manual sampling area, and the inner diameter is different from the inner diameter of the steam delivery pipe.

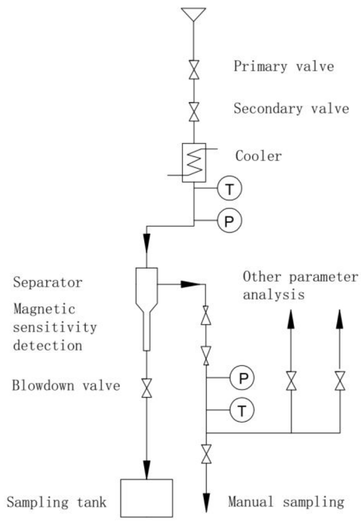

Figure 1 Work Flow Chart of On-line Separation System for Oxide Granules

MAGNETIC NONDESTRUCTIVE TESTING OF OXIDE GRANULES

Principle of Magnetic Testing

The oxide granules is mainly composed of Fe_2O_3 and Fe_3O_4, and the content of Fe_2O_3 accounts for about 16% - 25% [15,16]. The separator in the sampling system for oxide granules is of Austenitic stainless steel, a low-magnetic substance with a magnetic permeability of 1.0017. However, Fe_2O_3 and Fe_3O_4 in oxide granules are ferrimagnetic substances with the magnetic permeability of about 10 and 60 respectively, and belong to the ferromagnetic substances with magnetic permeability 10/60 times that of Austenitic stainless steel respectively. Since the magnetic properties of the oxide granules and the Austenite separator material are significantly different, the spatial magnetic field detection model of the oxide granules can be established based on the differences in the magnetic properties detected.

Spatial Magnetic Field Model of Oxide Granules

If a magnetic field is applied in the space where the Austenite separator is located, the computation formulas for magnetic induction of the oxide granules in the magnetic field environment are as follows:

$$B = \mu_0(H + M) \tag{4}$$

$$M = \chi H \tag{5}$$

In the formulas (4) and (5), B refers to the magnetic induction at the place where the oxide granules are piled; μ0 refers to the vacuum permeability; H refers to the intensity of the applied magnetic field; M refers to the magnetization of oxide granules; χ refers to the magnetic susceptibility of the oxide granules. Because the oxide granules are ferromagnetic substances, the magnetic susceptibility χ is much higher than that of Austenitic stainless steel pipes. Therefore, under the action of the spatial magnetic field, the presence of oxide granules in the separator will cause a large change in the magnetic induction in the surrounding space.

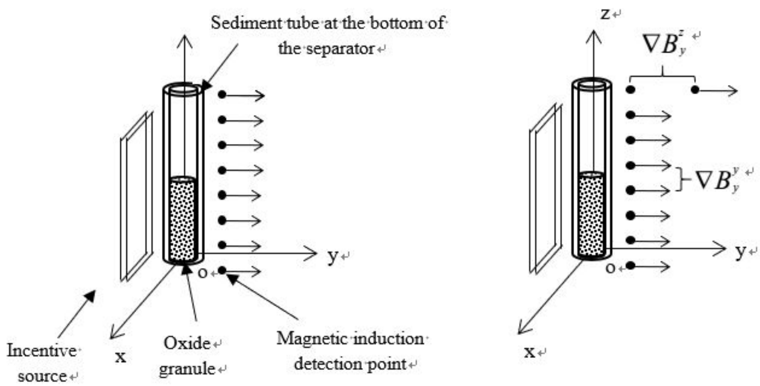

Figure 2 Spatial Magnetic Field Model of Oxide Granules in the Separator

Figure 3 shows the spatial magnetic induction detection model around the oxide granules in the constant magnetic field space. In this figure, the direction of the magnetic induction generated by the excitation source of constant magnetic field is parallel to the Plane XOY (radial magnetic induction). The magnetic induction component (axial magnetic induction) parallel to Z Axis is ignored in the model. The radial magnetic induction component can be divided into a magnetic induction component Bx along X Axis and a magnetic induction component By along Y Axis. The magnetic induction component By of the sidewall of the sediment tube is significantly stronger than Bx. Therefore, only the magnetic induction component By can be modeled.

According to the superposition of the magnetic induction, the magnetic induction components By of the detection points in the space are respectively generated by the excitation source and the magnetized oxide granules. The magnetic induction component generated by the excitation source at the detection point is By', and the magnetic induction component generated by the magnetized oxide granules at the detection point is By"; According to the computation formulas for magnetic induction:

$$B_y = B_y^{'} + B_y^{"} \tag{6}$$

$$B_y^{'} = \frac{N\mu_0 I}{4\pi r_n}(cos\theta_1 - cos\theta_2) \quad (7)$$

$$B_y^{"} = \frac{\varphi}{s} \quad (8)$$

In formula (7), μ_0 refers to the vacuum permeability, $\mu_0 = 4\pi * 10^{-7}$ H/m; I refers to the wire current in ampere (A); N refers to the number of turns of excitation source coils; r_0 refers to the distance between the measuring point and the energized wire (in m); θ1 and θ2 refer to the angles between the measuring point and the end point of the energized wire/current direction, in which θ1 is the acute angle while θ2 is the obtuse angle. In formula (8), Φ refers to the magnetic flux generated by the magnetized oxide granules at the detection point along Y Axis; s refers to the magnetic flux area.

The effects of whether the oxide granules exist or not on the magnetic induction component By along Y Axis is analyzed and compared. First, the magnetic induction distribution around the magnetized oxide granules is simulated, as shown in Fig. 4(a). The magnetic induction component along Y Axis of the surrounding space detection point is established as shown in Fig. 4(b).

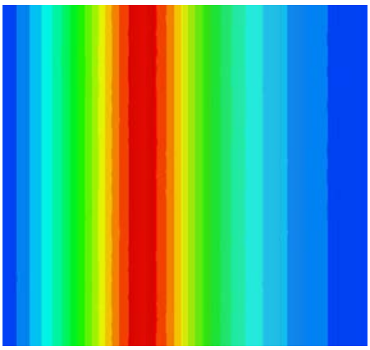

(a) Tube-side magnetic induction intensity distribution in empty tube

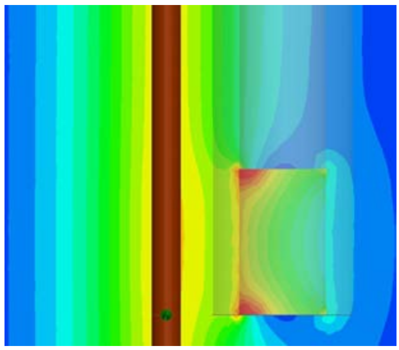

(b) Axial magnetic induction intensity distribution on the side of oxide scale

Fig.3 Axial magnetic induction intensity distribution on the side of the oxide particle

As can be seen from Fig. 3(a), when there is oxide scale particles in the tube, the positional magnetic induction intensity of the oxide scale particles in the tube is higher than that of the empty tube, and the position magnetic induction intensity of the non-oxidized particles in the tube is substantially the same as that of the empty tube, so By" is ignored for the spacial detection point without the oxide granules:

Position with oxide granules: $B_y = B_y^{'} + B_y^{"}$

Position without oxide granules: $B_y \approx B_y^{'}$

To estimate the accumulation position of the oxide granules more accurately, a spatial gradient of the parametric magnetic induction ($\nabla\vec{B}$) is introduced.

$$\nabla\vec{B} = \frac{\Delta\vec{B}}{\Delta d} \quad (9)$$

In formula (9), $\nabla\vec{B}$ refers to the spatial gradient of the magnetic induction; $\Delta\vec{B}$ is the variation of the magnetic induction in a certain direction; Δd refers to the spatial position variation in a certain direction, causing the spatial gradient variations of the magnetic induction component B_v along the Z Axis is ∇B_v^z (axial gradient). From formula (9), it can be inferred that the axial gradient ∇B_v^z of the magnetic induction component B_v in the spatial magnetic field where the oxide granules exist:

Position with oxide granules: $\nabla B_v^z = \nabla(B_v^{'} + B_v^{''}) \approx 0$ (10)

Boundary position with oxide granules: $\nabla B_y^z = \frac{B_y^{''}}{\Delta d}$ (11)

Position without oxide granules: $\nabla B_y^z = \nabla B_y^{'} \approx 0$ (12)

Detection System for Oxide Granules

This paper proposes a detection system for oxide granules based on the difference between the magnetic properties of the separator material and the oxide granules. The system includes an excitation system and a signal detection subsystem.

The excitation system consists of a DC source and excitation coils, mainly applying a magnetic field around the separator and the oxide scales. The separator material is of Austenitic stainless steel. The skin effect of the alternating magnetic field cannot penetrate the outer wall of the separator to magnetize the oxide granules, so the constant magnetic field generated by the DC source is selected as the excitation magnetic field.

The signal detection system includes the tunnel-type magnetic sensor, small signal noise-reduction amplifier circuit, signal transmission circuit and upper computer interface prepared by Labview. After the excitation system completes the magnetization of the separator and the oxide scales in the separator, the signal detection system detects the variations of the magnetic induction around the separator. The magnetic sensor used outputs a differential voltage signal with a sensitivity up to 25 mv/v/oe according to the variations of the magnetic induction. The relationship between the variations in magnetic induction (ΔB) and the output differential signal of magnetic sensor (Δv) is as shown in formula (5):

$$\Delta v = \Delta B \times v_s \times v_l \quad (13)$$

It can be known from formula (5) that, the variations of the differential voltage signal output from the magnetic sensor is proportional to the variations of the magnetic induction, and the variations of the magnetic induction around the separator can be measured by the variations of the differential voltage signal output from the sensor.

EXPERIMENTAL RESULTS AND ANALYSIS

The simulation analysis software can simulate the effects of oxide granules on magnetic induction under the action of a magnetic field. The simulation conditions are set according to the actual experimental parameters. The excitation source is set to the square winding coils with 60 turns of coils and the energization current of 0.3 A. The oxide granule conditions are set in a cylindrical region with a magnetic permeability of 10.

The experimental platform is built up by simulating the accumulation of oxide granules in the separator. The oxide granules are deposited in the separator sediment tube. The excitation source is placed on the one side of the separator sediment tube to form a constant magnetic field, and the detection device is placed on the other side of the separator sediment tube. The magnetic sensitivity detection device moves along the side wall of the separator sediment tube to detect the magnetic induction, and collects 40 sets of magnetic induction data covering each point on the side wall of the separator sediment tube in different oxide granule accumulation height of 0 - 180 mm after the application of the magnetic field. The variation curve of the magnetic induction at each signal acquisition point is shown in Fig. 4. As shown in Fig. 3, the spatial magnetic induction of the portion with oxide scale accumulation differs significantly from that of the potion without oxide scale accumulation, and the magnetic induction changes rapidly at the boundary position.

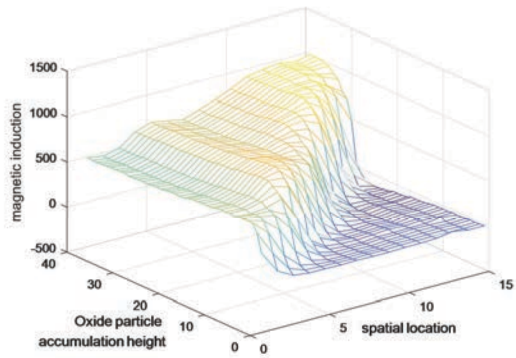

Fig. 4 Variation Curve of the Magnetic Induction

According to the above characteristics, a variation curve of the spatial gradient of the magnetic induction is shown in Fig. 5, depicting the gradient variation of the magnetic induction with the changes in the spatial position of the detection point. As shown in Fig. 6, as the spatial gradient varies, the variation of the magnetic induction at the positions with/without the oxide scale accumulation is relatively small, and the magnetic induction changes significantly with the spatial gradient at the boundary position.

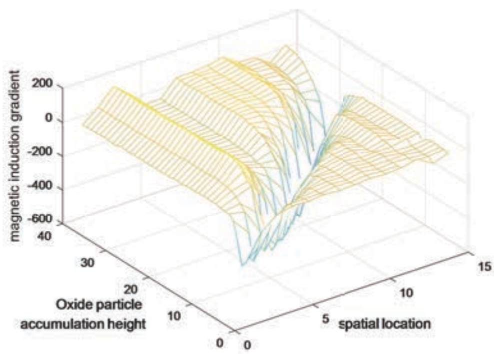

Fig. 5 Variation Curve of Spacial Gradient of Magnetic Induction

The effect test is conducted on 40 sets of oxide granule accumulation models at different heights. The test results are shown in Fig. 6.

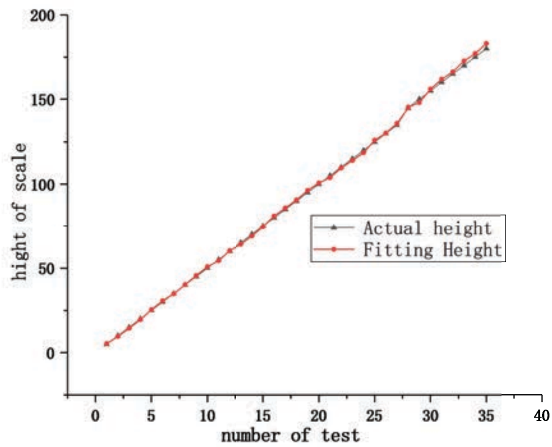

Fig. 6 Modeling Effect Test

The estimation of oxide scale accumulation has higher detection accuracy through the changes in magnetic induction of the magnetized oxide granules as the spacial gradient varies. The test error is less than 2%, which meets the requirements of industrial field test.

CONCLUSIONS

This paper proposes the on-line sampling system and device for oxide scales, which makes the oxide scale-vapor sample from the main steam pipeline form a liquid-solid two-phase flow after the temperature and pressure reduction, causes the oxide granules separated and deposited from the water through the separator and provides an opportunity to measure the oxide scale accumulation height.

This paper proposes a new multi-channel magnetic detection device for the accumulation of oxide granules. The laboratory test results shows that the detection error of the accumulation position of the oxide granules in the vertical tube of the separator is less than 2%.

Since the amount of oxide scales in the vapor-solid two-phase flow under the high temperature and pressure during the operation of the generator unit is small and less than the detection limit of the above device, the follow-up study will use the magnetic sensitivity matrix and the granularity testing method to further improve the detection accuracy.

ACKNOWLEDGMENTS

The study is funded by the research and development fund project (TP-18-TYK07) of Xi'an Thermal Power Research Institute Co., Ltd., China Huaneng Group Co., Ltd.

REFERENCES

[1] Long H.G. A new detection method for Oxidation Scales on Inner Surface of Austenitic Stainless Steel Tube Bends for Boilers. Journal of Chinese Society of Power Engineering, 2010,30(07):554-558.

[2] Ahmad J, Purbolaksono J, Beng L C. Failure analysis on high temperature superheater ineonel 800 tube. Engineering Failure Analysis, 2010,17(1):328-333.

[3] Liu Yacheng, Fan Weidong, Zhang Xiang, et al. High-Temperature Corrosion Properties of Boiler Steels under a Simulated High-Chlorine Coal-Firing Atmosphere. Energy & Fuels, 2017,31(4):4391-4399. 158-I 67.

[4] Zhang F.A., Zhu B.T. Application of Ultrasonic Technique in Measuring Oxide-layer Thickness in Boiler Heat-absorbing Tube Inspection. New Technology & New Process, 2014(09):117-120.

[5] Zhou Yongli, Lu Jintao, Gu Yuefeng. Research Progress of Surface Modification on Coal-fired Power Plant Boiler Tubes. Proceedings of the CSEE, 2017, 37(1): 149-160 (in Chinese).

[6] Purbolaksono J, Ahmad J, Beng L C, et al. Failure Analysis on a Primary Superheater Tube of a Power Plant. Engineering Failure Analysis, 2010,17(1).

[7] Ding K.Q., Zhao N. Study on the Stainless Steel Tube Oxide-scale Detection Technology in the Boiler. Nondestructive Testing, 2010,32(08):601-604.

[8] Zheng X.T., Yu H.W., Dong W.X. Detection Methods for Oxide Skin on Inner Heating Surface of Boiler Tubes. China Special Equipment Safety, 2016,32(03):49-52.

[9] Park H Y, Baek S H, Kim Y J, et al. Numerical and experimental investigations on the gas temperature deviation in a large scale, advanced low nox, tangentially fired pulverized coal boiler. Fuel, 2013,104(2): 641-646.

[10] Abe F. Research and development of heat-resistant materials for advanced use power plants with steam temperatures of 700 c and above . Engineering, 2015,1(2): 211-224.

[11] Xu Z.Y., Zhu J.Z., Yuan X.M., Lin W. Pulsed Eddy Current Testing for Thickness Measurement of Oxide Scales Accumulated in Austenitic Boiler Tubes . Nondestructive Testing, 2017,39(10):12-16.

[12] Liu Dingping. Research on Mechanisms for Forming and Spalling of Oxide Scales and Explosion-proof Technology of Ultra-supercritical Power Station Boilers [D]. South China University of Technology,2012.

[13] Peng X., Li X.H., Liu Y., Zhao Z.F., Ding H. Research on Detection of Accumulated Oxide at the Elbow of High Temperature Heating Surface Tubes by Acoustic Impulse Method. Proceedings of the CSEE, 2011,31(08):104-107.

[14] Palen J W, Breber G, Taborek J. Prediction of flow regimes in horizontal tube-sidecondensation. Heat Transfer Engineering, 1979, 1(2):10-12.

[15] Zhang N-q, Xu H, Li B-r, et al. Influence of the dissolved oxygen content on corrosion of the ferritic-martensitic steel p92 in supercritical water. Corrosion Science, 2012,56: 123-128

[16] Zhong X, Wu X, Han E-H. Effects of exposure temperature and time on corrosion behavior of a ferritic-martensitic steel p92 in aerated supercritical water. Corrosion Science, 2015,90: 511-521.